The Abdus Salam
International Centre for Theoretical Physics

United Nations
Educational, Scientific
and Cultural Organization

International Atomic
Energy Agency

H4.SMR/1775-18

"8th Workshop on Three-Dimensional Modelling of
Seismic Waves Generation, Propagation and their Inversion"

25 September - 7 October 2006

Inversion of Focal Mechanisms For Regional Stress Field Evaluation Application to fluid induced seismicity

F. H. Cornet

Institute de Physique du Globe de Paris
France

Inversion of Focal Mechanisms For Regional Stress Field Evaluation Application to fluid induced seismicity

F.H. Cornet
Institut de Physique du Globe de Paris

7th Workshop on three dimensional modeling of Seismic Waves Generation, Propagation and their inversion

Trieste; September 25– October 6; 2006

Table of content

One of the key variables involved in the understanding of deformation processes of the crust is stress. Because stresses are an essential boundary condition to many an applied engineering problem, be it mining, civil or petroleum, most techniques for determining stresses at depth have involved measurements in boreholes. But deformation processes in the crust involve depths that are generally not accessible to boreholes. Hence, methods based on remote observations are being developed for determining the stress field at depths greater than a few kilometers. Presently two methods are being used routinely, the analysis of shear wave polarization (shear wave splitting analysis) and the inversion of double couple focal mechanisms.

This presentation first recalls some elementary principles for rock mass stability analysis. Then two methods of fault plane solution inversions are presented. Examples where they have been applied are discussed. They help precise conditions that must be satisfied for the methods to be valid.

1. Some Elementary Rock Mechanics Principles

(Typing convention: bold letters are vectors, bold italic letters are tensors)

1.1 The stress vector and the Mohr representation

The stress vector is defined by:

$$\mathbf{t} = \boldsymbol{\sigma}\mathbf{n}, \qquad (1)$$

t is the stress vector acting on a surface element S, with normal **n** and unit area, on which exists at all points the stress tensor **σ.** In this expression, the unit area is assumed to be small as compared to distances for which stress variations are significant so that stress gradients may be neglected. Hence, all components of the stress tensor are constant.

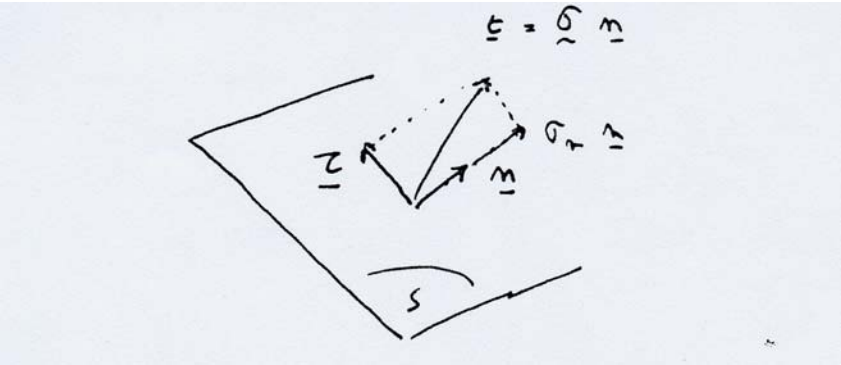

The stress vector has a normal component, (called the normal stress (scalar)) :

$$\sigma_n = \boldsymbol{\sigma}\mathbf{n} \cdot \mathbf{n} \qquad (2)$$

and a shear component (vector):

$$\boldsymbol{\tau} = \boldsymbol{\sigma}\mathbf{n} - (\boldsymbol{\sigma}\mathbf{n} \cdot \mathbf{n})\,\mathbf{n} \qquad (3)$$

The stress tensor $\boldsymbol{\sigma}$ is symmetrical when there exists no moment in any small volume of the body under consideration. Hence it is characterized by six components, i.e. σ_{ij} , with i, j = 1,2,3, the components in any frame of reference, or its eigen values (σ_1 , σ_2 , σ_3 , with the classical convention $\sigma_3 < \sigma_2 < \sigma_1$) and its eigen vectors $\mathbf{e_1}$, $\mathbf{e_2}$, $\mathbf{e_3}$. The eigen vectors are defined by three independent angles, called the Euler angles, namely ψ , φ and θ. ψ and φ correspond to the azimuth and dip of $\mathbf{e_1}$ in the frame of reference (defined by the unit vectors $\mathbf{I_1}$, $\mathbf{I_2}$, $\mathbf{I_3}$, which may be the geographical frame of reference so that North is $\mathbf{I_1}$, East is $\mathbf{I_2}$, and $\mathbf{I_3}$ is vertical positive downward). Once the frame of reference has been rotated so that $\mathbf{I_1}$ becomes $\mathbf{e_1}$ and $\mathbf{I_2}$ becomes $\mathbf{I_2'}$, θ is the rotation about $\mathbf{e_1}$ which brings $\mathbf{I_2'}$ parallel to $\mathbf{e_2}$.

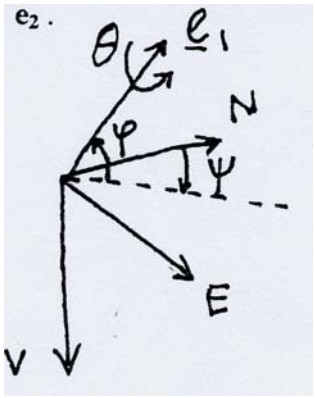

For $\mathbf{n}$ parallel to any eigen vector, $\boldsymbol{\tau} = \mathbf{0}$. Given that σ_n and $|\boldsymbol{\tau}|$ vary with the orientation of $\mathbf{n}$, the set of all couples of values σ_n and $|\boldsymbol{\tau}|$ corresponds to the area limited by the three Mohr circles as shown on figure 1.

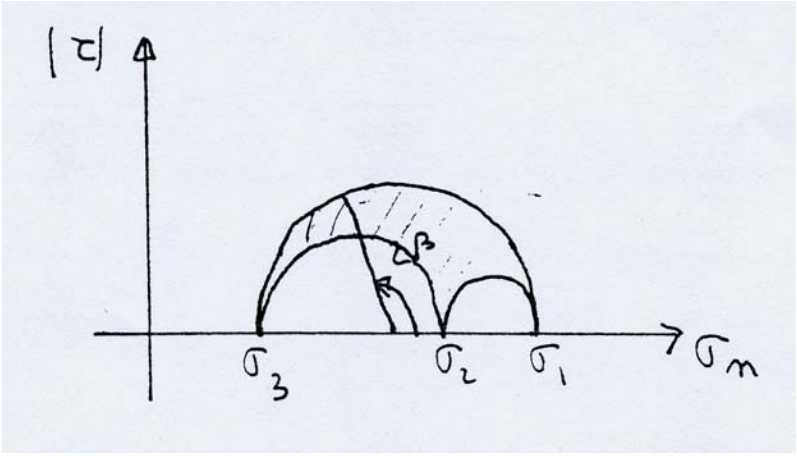

Figure 1 : The Mohr Circles. Each circle corresponds to the set of values for σ_n and $|\boldsymbol{\tau}|$ when $\mathbf{n}$ is perpendicular to either $\mathbf{e_1}$, $\mathbf{e_2}$ or $\mathbf{e_3}$.

When $\mathbf{n}$ is perpendicular to $\mathbf{e_2}$, the values for σ_n and $|\boldsymbol{\tau}|$ are :

$$\sigma_n = (\sigma_1 + \sigma_3) / 2 + [(\sigma_1 - \sigma_3) / 2] \cos(2\beta) \qquad (4)$$

$$|\boldsymbol{\tau}| = [(\sigma_1 - \sigma_3) / 2] \sin(2\beta) \qquad (5)$$

where β is the angle between the normal **n** and $\mathbf{e_1}$ (see figure 1)

The rock mass is globally in equilibrium (i.e. in between slip events, whether seismic or aseismic), so that the stress components must satisfy the equilibrium equation:

$$\sigma_{ij,i} + \rho\, b_j = 0 \; ; \; i, j = 1,3 \qquad (6)$$

with $\mathbf{b} = -\, g\delta_j 3\, \mathbf{I}_j$, the gravity, and ρ the rock density. Typically, for rocks, the vertical component of the vertical stress gradient is of the order of 2 to 3 mPa per 100 meters.

The concept of **Elementary Representative Volume** for the definition of Stress in geomechanics.

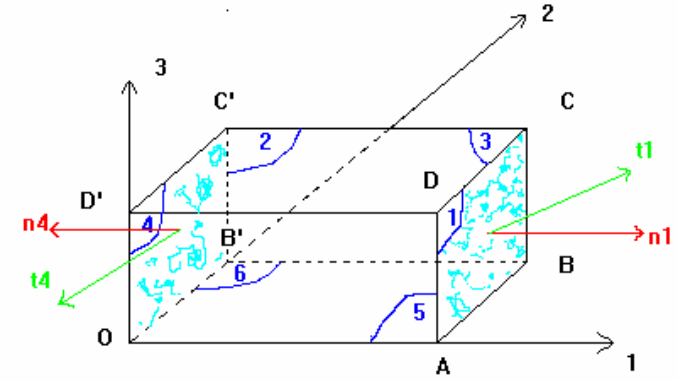

The Elementary Representative Volume must be small enough for the stress gradient to be neglected so that forces on opposed faces are equal in magnitude.

1.2 Griffith Fracture criterion and Irwin's basic fracture modes

Fracture always corresponds to the extension of a pre-existing surface of discontinuity in a material called a microcrack. This extension implies the formation of a surface increment that requires a quantity of energy, called surface energy, proportional to the area of the newly created surface (Griffith, 1921). The extension **ds** (**ds** = **n** da, where **n** is the unit normal to the surface **ds** of area da) of a fracture with surface **s**, implies an increment of surface energy for the rock ΔD (**ds**) such that :

$$\Delta D\,(\mathbf{ds}) = 2\,\gamma\,da, \qquad (7)$$

γ is the surface energy of the material per unit area. The quantity 2 in equation (7) reflects the fact that the surface increment **ds** exhibits two sides, each with an area da.

During fracturing, conservation of energy implies (when neglecting thermal effects):

$$\Delta W(\mathbf{ds}) = \Delta E(\mathbf{ds}) + \Delta T(\mathbf{ds}) + \Delta D(\mathbf{ds}) \qquad (8)$$

Where ΔW(**ds**), ΔE(**ds**) and ΔT(**ds**), are respectively the work of external forces , the change in elastic energy and the change in Kinetic energy during the formation of **ds.**

Before crack extension, the body is assumed to be at rest so that there is no kinetic energy and the criterion for fracture e initiation is :

$$\Delta W(\mathbf{ds}) - \Delta E(\mathbf{ds}) = \Delta D(\mathbf{ds}) \qquad (9)$$

One defines the quantity $G = \lim_{da \to 0} \left[\Delta W(ds) - \Delta E(ds)\right] / da$ as the Strain Energy Release Rate.

Evaluating G is an elasticity problem. Fracture occurs when G reaches the critical value 2 γ. If it increases with fracture propagation, the fracturing process is unstable, while if it decreases, the fracturing process is stable and work must be supplied to the system in order to extend further the fracture. When G remains constant during fracture propagation, the fracturing is called quasistatic. A typical example of quasistatic fracture propagation is hydraulic fracturing, as discussed here after.

Because the variation in elastic energy $\Delta E(\mathbf{ds})$ is entirely dominated by stress concentration close to the fracture tip, it can be evaluated by analyzing the stress field only close to this fracture tip. For this purpose, Irwin (1958) defines a local frame of reference for analyzing the surface discontinuity **ds** (see fig.**)**. The 1 axis is in the plane of the fracture and is normal to the fracture front. The 2 axis is also in the fracture plane but is parallel to the fracture tip. The 3 axis is normal to both previous axes and therefore is normal to the fracture plane.

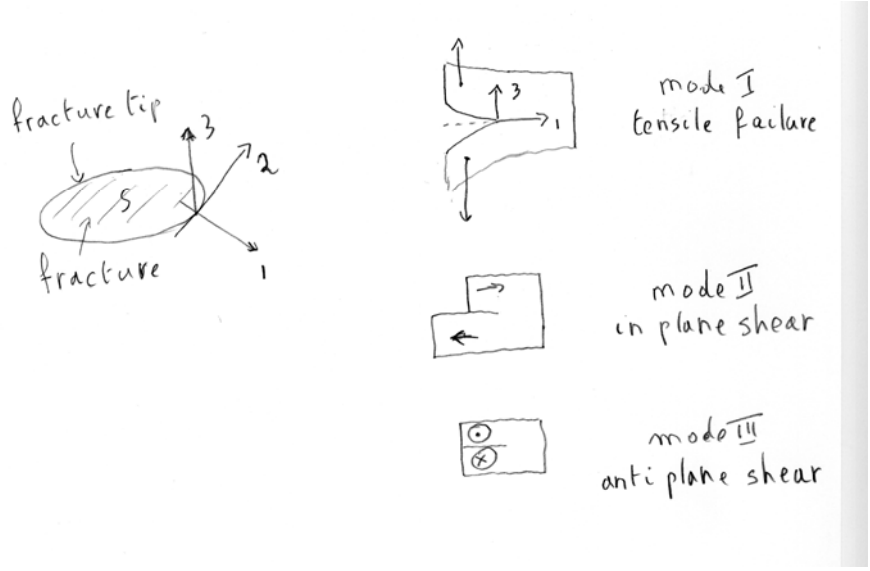

Within this local frame of reference, Irwin defines three basic modes of failure. Mode 1, in which **ds** has zero components along the 1 and 2 axis. It corresponds to a pure tension. Mode 2 has zero components along axes 2 and 3 and is called in plane shear. Mode 3 has zero components along axis 1 and 3 and is anti plane shear.

1.3 Principle of hydraulic fracturing

Hydraulic fracturing occurs when the fluid pressure that is applied in a cavity, whether a borehole, a magmatic chamber or the pore space of rock, exceeds the tensile strength of the rock. Hydraulic fractures are “mode 1” fractures and it can be shown from the principal of minimum potential energy that they develop normal to the minimum

principal stress direction. We describe as an example the development of hydraulic fracturing in a vertical borehole.

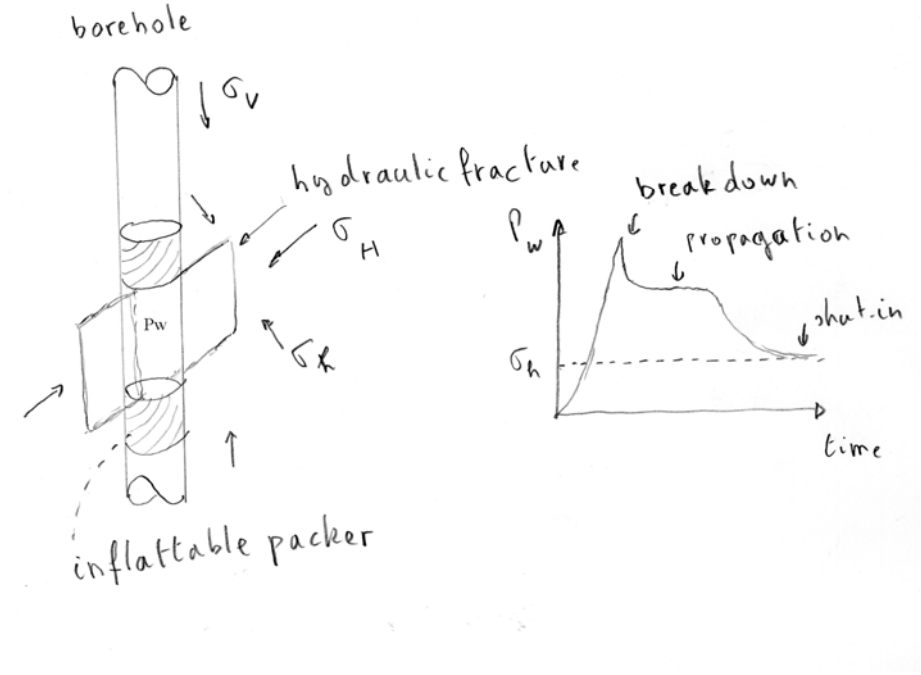

The stress field at distance ρ from the borehole axis, expressed in cylindrical coordinates as a function of the far field stress state is :

$$\begin{aligned}
\sigma_{\rho\rho} &= \left(1-r^2/\rho^2\right)\left(\sigma_{11}+\sigma_{22}\right)/2 + \left(1-4r^2/\rho^2+3r^4/\rho^4\right)\left[1/2\left(\sigma_{11}-\sigma_{22}\right)\cos 2\theta + \sigma_{12}\sin 2\theta\right] \\
\sigma_{\theta\theta} &= \left(1+r^2/\rho^2\right)\left(\sigma_{11}+\sigma_{22}\right)/2 - \left(1+3r^4/\rho^4\right)\left[1/2\left(\sigma_{11}-\sigma_{22}\right)\cos 2\theta + \sigma_{12}\sin 2\theta\right] \\
\sigma_{zz} &= \sigma_{33} - 4\nu\left(r^2/\rho^2\right)\left[1/2\left(\sigma_{11}-\sigma_{22}\right)\cos 2\theta + \sigma_{12}\sin 2\theta\right] \\
\sigma_{\theta z} &= \left(1+r^2/\rho^2\right)\left(\sigma_{23}\cos\theta - \sigma_{31}\sin\theta\right) \\
\sigma_{z\rho} &= \left(1-r^2/\rho^2\right)\left(\sigma_{31}\cos\theta + \sigma_{32}\sin\theta\right) \\
\sigma_{\rho\theta} &= \left(1+2r^2/\rho^2-3r^4/\rho^4\right)\left[1/2\left(\sigma_{22}-\sigma_{11}\right)\sin 2\theta + \sigma_{12}\cos 2\theta\right]
\end{aligned} \tag{10}$$

Given that the borehole pressure Pw generates a tensile stress $\sigma_{\theta\theta} = -P_w$ at the borehole wall, the pressure required to induce a hydraulic fracture is :

$$\sigma_{\theta\theta} = -\sigma_H + 3\,\sigma_h - P_w + \sigma^T \tag{11}$$

Where, σ_H and σ_h are respectively the far field maximum and minimum horizontal principal stress components and σ^T is the rock tensile strength.

From equation (10) it ma be observed that the tangential stress component reaches its maximum value at the angular coordinate π/2 from the direction of the hydraulic initiation. This is further discussed in field examples described in the later part of the lecture.

1.4. Stress failure in rock masses under compressive stress fields

A rock mass involves both, intact rock volumes and preexisting fractures and faults. Hence failure criteria must address both the failure of intact rocks and that of preexisting weakness planes.

1.4.1 Criteria of failure for intact rocks

Once the minimum principal stress gets larger than 2 to 5 mPa, failure in compression involves the formation of macroscopic shear zones. Various stress criteria have been proposed to characterize the stress condition that must be met for these shear zones to appear.

The Tresca criterion.

$$(\sigma_1 - \sigma_3) = K \qquad (12)$$

The Tresca criterion assumes that failure occurs when the maximum differential stress in the material reaches a critical value, which is independent of the minimum principal stress magnitude. Note (see the Mohr representation on figure 2) that this assumes that the corresponding shear zone is inclined 45 ^{o} to the maximum stress orientation. Laboratory work has shown that for rock, this is valid only for very soft material like clay or salt, or for stress and temperature conditions which, for most rocks, correspond to depths greater than 20 km. It is not valid for seismicity observed in the upper 10 to 15 km.

The Coulomb criterion and the Mohr envelope

$$|\tau| = \mu \sigma_n + C_0 \qquad (13)$$

μ is called the internal friction angle and C_0 is called the cohesion. This criterion has been found to be valid for limited stress domains. For large stress domains the so-called friction angle decreases as the minimum principal stress increases. It gets close to 0 when both the minimum principal stress and the temperature gets large so that the criterion of failure gets close to the Tresca criterion (see figure 2). Hence the failure criterion is not represented by the simple linear law proposed by Coulomb but may be approached by a parameterization of the so-called Mohr envelope. This envelope corresponds to the set of values for $|\tau|$ and σ_n for which failure occurs. It is often assumed to be independent of the intermediate principal stress magnitude, so that failure surfaces are assumed to be parallel to the intermediate principal stress direction. However recent laboratory work, in particular by Haimson et al.(1997), has shown this not always to be valid. This will not be discussed further here for it has no incidence for our discussion

The effective stress principle

When the rock mass is saturated with a fluid under pressure, experiments show that, under compressive conditions, failure is controlled by so-called effective stresses rather than by total stresses. The effective stress tensor $\boldsymbol{\sigma'}$ is defined as :

$$\boldsymbol{\sigma'} = \boldsymbol{\sigma} - P\,\mathbf{I} \qquad (14)$$

where **I** is the unit tensor and P is pore pressure. Note that, on the Mohr diagram, subtracting P to all diagonal terms of the stress tensor matrix corresponds to shifting all Mohr circles to the left, leaving unchanged their radius.

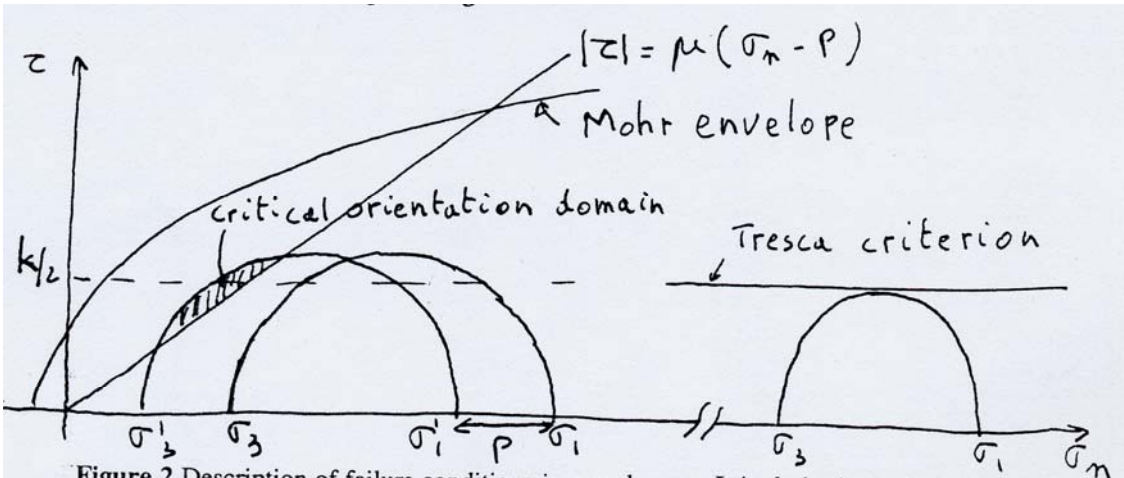

Figure 2 Description of failure conditions in a rock mass. It includes both, failure in the intact rock and failure along preexisting weakness planes as expressed in terms of effective stresses.

1.4.2. Failure along preexisting weakness planes

It is generally accepted that failure along preexisting planes is well represented by Coulomb's friction law, expressed in terms of effective stresses :

$$|\tau| = \mu (\sigma_n - P) + C_0 \qquad (15)$$

Byerlee (1978) has shown that for most rocks the friction coefficient ranges from 0.6 to 0.9. For wet rocks, most field data point out to values for the friction coefficient ranging from 0.6 to 0.8 and negligible cohesion, so that the failure along preexisting weakness planes at depths greater than a few hundred meters is well represented by Byerlee's law :

$$|\tau| = \mu (\sigma_n - P); \ 0.6 \leq \mu \leq 0.8 \qquad (16)$$

It may be noted that $|\tau|$ and σ_n are computed for the corresponding weakness plane. Hence, it is possible for the Mohr circles to intersect the line which corresponds to Byerlee's law and yet to observe stability. This is possible if there is no preexisting plane in the critical orientation domain. However, it has been argued that fractured rock masses have a long enough tectonic history that there always exists a plane with critical orientation. Hence it is often considered that the Mohr circle representing the stress at any point in the rock mass is at most tangent to the straight line which corresponds to Byerlee's law.

Let us observe that, because sliding depends on effective stresses, planes with a great variety of orientations may slip if the local pore pressure becomes large enough, as pointed out by McKenzie (1969).

The equilibrium of rock masses is classically analyzed with a Mohr diagram as shown on figure 2. Note that failure along preexisting weakness planes is the controlling

phenomenon in most cases. An important difference between the development of new shear zones and the slipping along preexisting weakness planes, is that the orientation of new shear planes may be determined from the principal stress directions, if the corresponding internal friction coefficient is known (the Mohr circle at rupture is tangent to he Mohr envelope), but this is not true for preexisting weakness planes, given the role of pore pressure.

Because pore pressure is unknown, tt is concluded that seismicity occurring in the upper 15 to 20 km of the crust involves fracture planes that make an unknown angle with respect to the principal stress directions.

In the above discussion, the friction angle and the cohesion are isotropic so that, if slip occurs, it will occur in the direction of the resolved shear stress (**τ)** in the plane (Bott, 1959). But this direction of resolved shear stress depends on the relative orientation of the slip plane with respect to the principal directions as well as on the relative magnitude of principal stress components. This is the basic principle underlying stress determinations from a collection of fault planes solutions.

2. Inversion of double couple focal mechanisms for stress determination

2.1 data produced by Fault plane solutions

Focal mechanisms of pure shear faults (pure double couples, no significant dilatancy), yield for both nodal planes the dip and azimuth of the plane (d and a) as well as the slip direction in the plane (rake angle r of slip vector **s**) when it corresponds to the fault plane.

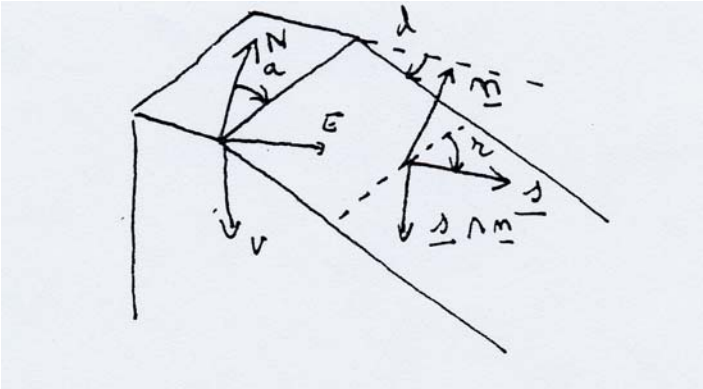

As may be observed in figure 2, during a fluid injection, the pore pressure rises may induce some seismic activity. Preexisting fracture planes that were at equilibrium before the fluid injection may get unstable if the corresponding effective normal stress is lowered enough that the shear stress supported by the plane becomes larger or equal to the shear strength supported by the plane (taken generally equal to friction). Hereafter are typical focal mechanisms observed during a large scale fluid injection.. Because the monitoring seismic network exhibits a limited number of stations, many a nodal plane is ill defined.

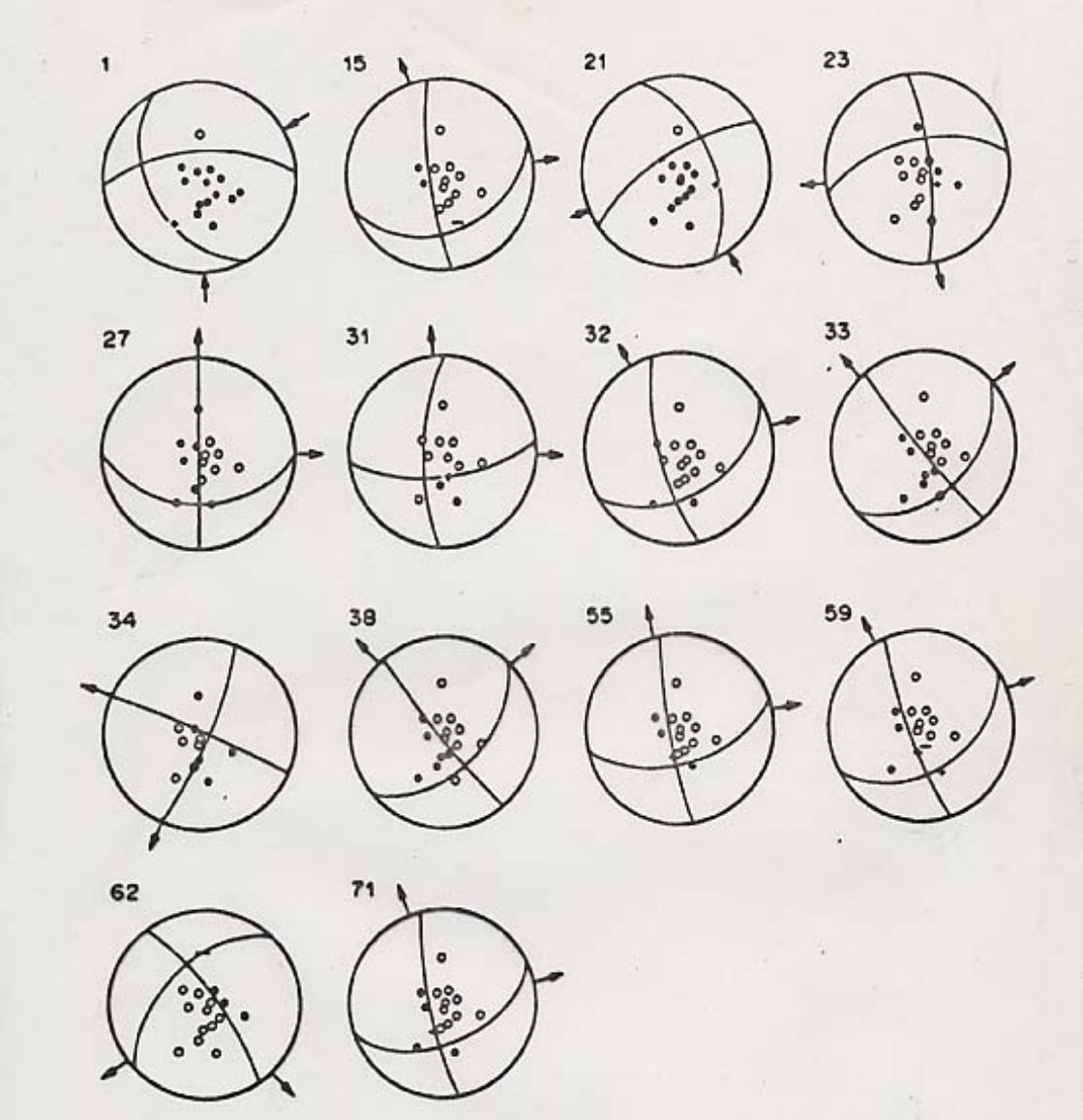

Focal mechanisms of induced seismicity during the initial reservoir development

Open dots correspond to dilation, black dots to compression lower hemisphere representation

For many of the focal mechanisms; it is impossible to identify which of the two nodal planes is the actual fault plane, if only the polarity of P waves is considered. The method proposed by Zollo and Bernard (1989, 1991) for determining focal plane solutions conducts an exhaustive search of all possible solutions and each solution is associated with a probability. Hence solutions with 60 %, 90 % and 99 % confidence

levels are determined. These confidence level domains are used then to determine the corresponding uncertainty associated with the various angles determination.

Note that when enough three components stations are being used, the radiation pattern for S waves help identify the fault plane. In the following, it is considered that the fault plane has not been identified so that both nodal planes are equally likely to be the fault plane. Hence for each focal mechanism,

a set of 12 values is identified : (a_1, d_1, r_1, εa_1, εd_1, εr_1 , a_2, d_2, r_2, εa_2, εd_2 , εr_2).

It is customary to identify P and T axis with focal mechanisms. These are inclined 45^o with respect to the nodal planes. It has been proposed sometimes to associate these axes respectively with the maximum and minimum principal stress direction. It should be noted here that, only when failure occurs according to the Tresca failure criterion (i.e. for very deep earthquakes) is this proposition valid. Hence this proposition is erroneous for most seismic events of the upper crust since either these correspond to the reactivation of preexisting weakness planes, or the newly formed shear zones are inclined by less than 45^o with respect to the maximum principal stress orientation.

2.2 Determination of the regional stress field from focal mechanisms

Gephart and Forsyth's approximate method

The method (Gephart and Forsyth, 1984) is based on the following assumptions :

1. Slip occurs parallel to the direction of the resolved shear stress;

2. All seismic events are distant enough from each other that the stress perturbation induced by each event does not alter the stress field for other events;

3. The original stress field is uniform within the volume sampled by the various events.

Validity of hypothesis 1 implies that the shear strength in all planes is isotropic while hypothesis 3 implies that events are not too distant from each other so that stress gradients may be neglected. This has implication for the depth ranges of events considered for a single inversion.

Because focal mechanisms yield only the direction (and sense) of slip and not the magnitude, the stress tensor cannot be fully determined.

Only four parameters are determined : the three Euler angles and an aspect ratio R defined as :

$$R = (\sigma_2 - \sigma_1) / (\sigma_3 - \sigma_1) \qquad (12)$$

So that $0 \leq R \leq 1$. Indeed, the stress at any point may be rewritten :

$$\boldsymbol{\sigma} = \sigma_1 \mathbf{I} + (\sigma_3 - \sigma_1) \mathbf{T} \qquad (13)$$

with :

$$T_{ij} = \begin{pmatrix} 0 & 0 & 0 \\ 0 & R & 0 \\ 0 & 0 & 1 \end{pmatrix}$$

so that **T** is characterized by 4 parameters (ψ , φ , θ , R). Note that ψ ranges from 0 to 360 ^{o}, while the range for φ is 90^{o} and that for θ is 180^{o}. Hence, the complete set of solutions for T is fairly limited and it can be fully explored with a grid search method. The solution is that which fits best the collection of focal mechanisms.

Let us determine now the condition for **T** to be consistent with a given focal mechanism, i.e. the tensor **T** for which the resolved shear stress $\boldsymbol{\tau_0}$ on a fault plane is parallel to the observed slip vector **s**. First it will be noted that $\boldsymbol{\tau_0} \cdot \mathbf{s} > 0$.

We consider now two frames of reference : the first one (Q) is associated with the eigen vectors of T. The second one (Q') is associated with the fault plane (**n** , **s** $\wedge$ **n** , **s**).

Let $\boldsymbol{\beta}$ be the orthogonal tensor which rotates Q to Q'. It may be observed that in Q', the stress component σ'_{12} is null. Hence, given the definition of Q, we obtain :

$$\sigma'_{12} = \sigma_1 \beta_{11} \beta_{21} + \sigma_2 \beta_{12} \beta_{22} + \sigma_3 \beta_{13} \beta_{23} = 0 \qquad (14)$$

so that

$$R = (\sigma_2 - \sigma_1) / (\sigma_3 - \sigma_1) = - \beta_{13} \beta_{23} / \beta_{12} \beta_{22} \qquad (15)$$

For a given fault plane defined by the triplet (a, d, r), and given a tensor **T** with Euler angles ψ , φ , θ, there is a unique value of R which fits the direction of slip in the corresponding plane. This is taken to advantage for identifying both the best solution $\mathbf{T_s}$ for the given set of focal mechanisms and its domains of confidence level.

The idea is to explore the set of all possible solutions and to identify that which fits best observations, namely the tensor, which yields resolved shear stress directions closest to observed slip vector directions.

The problem is three folds :

1. Identify for each focal mechanism which nodal plane is the fault plane;
2. For all focal mechanisms define a measure of their misfit with a given tensor **T.**
3. Identify the best solution and associated confidence level domains.

The measure of misfit and the identification of fault planes

It has been proposed sometimes to characterize the misfit between a given fault plane and a given tensor **T** by the angle between the shear stress resolved on that plane and the observed slip vector. But this assumes that the fault plane is known exactly while in reality this is not the case as mentioned here above. Gephart and Forsyth (1984) proposed to consider as measure of misfit, for any given plane, the smallest rotation which brings **s** parallel to the resolved shear stress in the plane (τ). They observe that this misfit is a well behaved function so that it suffices to consider only three rotations axis, namely **n,** **s** $\wedge$ **n** and **s.**

The rotation angles are computed according to equation (15) once Q' has been replaced by the frame of reference Q" that corresponds to the rotated Q' :

$$\mathbf{Q}'' = \mathbf{A}(i)\,\mathbf{Q}' \qquad (16)$$

where **A**(i) is the orthogonal tensor corresponding to rotations about **n**, **s** ∧ **n** or **s** . The angles of rotation are given here below **:**

Table 1

Expressions for rotations about axes of fault plane geometry.

Rotation axis	Algorithm	Period
n	$\theta = -\tan^{-1}\left[\dfrac{RB_{12}B_{22} + B_{13}B_{23}}{RB_{12}B_{32} + B_{13}B_{33}}\right]$	Π
s ∧ **n**	$\theta = \tan^{-1}\left[\dfrac{RB_{12}B_{22} + B_{23}B_{13}}{RB_{22}B_{32} + B_{23}B_{33}}\right]$	Π
s	$\theta = \dfrac{1}{2}\tan^{-1}\left(\dfrac{2}{k}\right)$ where $k = \dfrac{R(B_{12}^2 - B_{22}^2) + B_{13}^2 - B_{23}^2}{RB_{12}B_{22} + B_{13}B_{23}}$	$\dfrac{\Pi}{2}$

For any given **T** and any focal mechanism six rotation angles are computed : 3 for the first nodal plane and 3 for the second nodal plane. The nodal plane which yields the smallest rotation is chosen as fault plane and the measure of misfit for the corresponding plane is the smallest rotation. Hence, the misfit value associated to any given $\mathbf{T}^{(i)}$, is the sum of the misfit measures for all focal mechanisms. It is given by :

$$m_i = \sum_{k=1}^{N} \min(x_k^l, l = 1,6) \qquad (17)$$

where x_k^l is the l^{th} rotation for focal plane solution k, $1 \leq k \leq N$, for N focal mechanisms.

The solution is the tensor for which m_i is minimum. The corresponding value for the misfit is noted m_{min}. Here, the L_1 norm has been chosen rather than a least squares norm. Indeed, the choice of the nodal plane as fault plane is either right or wrong so that the error associated with the rotation angle determination does not obey a Gaussian law.

It has been proposed (Julien and Cornet, 1987) to introduce weight factors in the misfit function by dividing the minimum rotation angle by the uncertainty on the orientation of the nodal plane as defined by the focal mechanism determination. Also, when the rotation angle is larger than the solid angle that corresponds to the 90 % confidence level for the fault plane orientation, the focal mechanism is considered to be heterogeneous with the corresponding tensor. Then the quality of the solution is defined not only by the misfit value but also by the number of inconsistent data. Indeed, it may be argued that a solution which requires very small rotation angles but is heterogeneous with more than 50 % of the data is not satisfactory.

Let m_{50} and m_{90} be the values for the bounds of the misfit function which characterize respectively the 50 % and the 90 % confidence levels. For the L1 norm, Parker and McNutt (1980) have showed that these bounds may be defined with respect to the best solution as :

$$m_{90} = \{ [1.645(\pi/2-1)^{1/2} N^{1/2} + N] / (N-k)\} m_{min} \qquad (18)$$

and

$$m_{50} = \{ [0.676(\pi/2-1)^{1/2} N^{1/2} + N] / (N-k)\} m_{min} \qquad (19)$$

where k is the number of parameters in the model (here k= 4) and N is the total number of focal mechanisms.

Hence, all solutions for which the misfit m_i is found to be smaller than either m_{50} or m_{90} are plotted on a stereo net. The contour plot of these solutions identifies the 50 and 90 % confidence levels.

Once the approximate solution and its associated confidence levels are known, fault planes have been identified for each focal mechanism. Cornet and Julien (1987) have proposed a method based on a least squares method for identifying the best solution, once the approximate solution is known. However, experience has shown that this refining of the solution is not necessary for the solution remains within the 50 % confidence level domain. It suffices to run the approximate method with a finer grid restricted to the 90 % confidence level domain.

Stress determination in large volumes

When inverting for tensor **T,** it is assumed that the stress is uniform throughout the volume sampled by the various focal mechanisms. But, if only because of gravity, it is known that the stresses vary with depth and possibly also laterally. Hence the question arises as to the validity of this hypothesis.

Interestingly, most stress field measurements have shown that the stress varies linearly with depth. Further, as shown by Mc Garr (1980), when there is no lateral stress variation, the vertical direction is principal. Hence, in many a situation, the stress field may be written :

$$\sigma(x_3) = \sigma(x_c) + (x_3 - x_{3c})\, \alpha \qquad (20)$$

where $\sigma(x_3)$ is the stress at depth x_3, $\sigma(x_c)$ is the stress at the reference depth x_c (6 independent components) and α is the vertical stress gradient (six independent components which reduce to 4 independent components, namely the three eigen values and the orientation of one of the horizontal eigen vectors, when there is no lateral stress variation).

Equation (20) has revealed very useful for interpreting direct stress measurements in boreholes. Indeed, it is usually found that close to ground surface many perturbations of the stress field exist which nay be lumped as a fixed term for a given depth interval. But, as depth gets larger, the gradient term becomes more significant so that, when depth gets greater than 1 km, it may be considered that the vertical stress gradient dominates the stress field and that the constant term may be neglected. When this is the case, then the stress field can again be simplified so as to be characterized by only four parameters,

namely the three Euler angles and the R aspect ratio. However, now, R describes the aspect ratio of the vertical stress gradient and not the complete stress tensor at depth z ;

$$R = (\alpha_2 - \alpha_1) / (\alpha_3 - \alpha_1) \qquad (21)$$

Given that usually the rock mass density α_3, is rather well known, the determination of the ratio R provides constraints on the relative variations of both horizontal stress components when there is no lateral stress variation.

This observation opens the door now to a possibility of extrapolating borehole stress determinations, which are usually conducted in the upper kilometer of the crust, down to depths of natural microseismic activity. This is possible provided the stress gradient is continuous and stable for the complete depth interval. Hence the mapping of the complete stress field at the scale of the crust may become realistic, when combining borehole data and focal mechanisms of natural seismicity.

3. Other methods for stress determination at great depth : Borehole breakouts, drilling induced fractures, Hydraulic Fracturing and HTPF

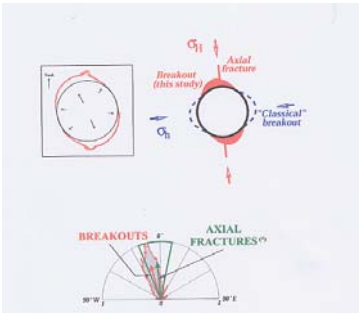

- Tangential stress at the borehole wall

$\sigma_{\theta\theta} = (\sigma_h + \sigma_H) - 2(\sigma_H - \sigma_h)\cos 2\theta - P_b -$
$f(P_0) - \alpha E \Delta\theta / (1-\nu) - 3/8\ \Delta\alpha E/(1-\nu)\ \Delta\theta$

Where $\Delta\alpha$ is the mismatch between thermal expansion coefficients (solution for square inclusion in an homogeneous matrix)

- Time dependency of cooling :
  - Slow cooling yields borehole elongation (thermal breakouts),
  - fast cooling yields macroscopic thermal cracking

Breakouts and tensile induced fractures are well detected with borehole imaging tools such as the Ultrasonic borehole imager or the Electrical Formation Imager.

Ultrasonic imaging (UBI)

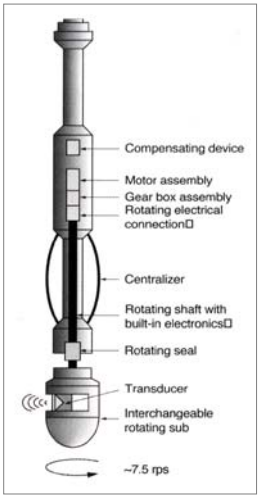

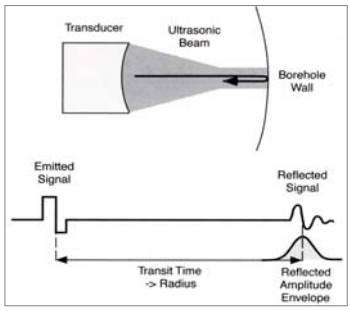

Hydraulic Fracturing (HF). When the borehole is parallel to a principal stress direction (vertical borehole in a rock mass in which the vertical direction is a principal stress direction), the Hydraulic Fracturing method discussed in section 1.3 yields a very reliable method for measuring the *in situ* stress field. Indeed, because the fracture is normal to the horizontal minimum principal stress direction, identification of its image, at the wellbore provides a direct measurement of the Maximum Horizontal principal stress direction. Analysis of the breakdown pressure yields a first relationship between the horizontal principal stress magnitudes and the rock tensile strength (supposed to be known from laboratory tests). After propagating the fracture outside the domain of influence of the well bore, the normal stress acting onto the fracture is the natural minimum principal stress Hence, when pumping is stopped, the fracture stops propagating till the fluid pressure, inside the fracture, is equal to the normal stress acting on the fracture, i.e. the minimum principal stress magnitude. This is called the shut in pressure and is taken as equal to the minimum principal stress magnitude. Thereafter, the maximum principal stress magnitude may be derived from the breakdown pressure equation.

HTPF method; the Hydraulic Tests on Preexisting Fractures (HTPF) method is somewhat similar to Hydraulic Fracturing, except that the injection flow rate is adjusted so as to reopen preexisting fractures that have been identified before hand by an electrical borehole imaging technique. Electrical imaging is chosen rather than acoustic imaging for it yields some qualitative information on the hydraulic conductivity of the fracture. Analysing relationship between injected flow rate and borehole pressure provides means to identify the pressure required to just open the fracture, i.e. the pressure value that is just equal o the normal stress acting onto the fracture. In principle, when fractures with at least six different orientations are tested, the relationships provided by equation (2) are inverted for getting all six stress components. In practice , generally only two or thressmain fracture orientations are observed and inversion is conducted with the additional hypothesis that the vertical direction is principle..

Typical hydraulic fracture records, for the HTPF method.

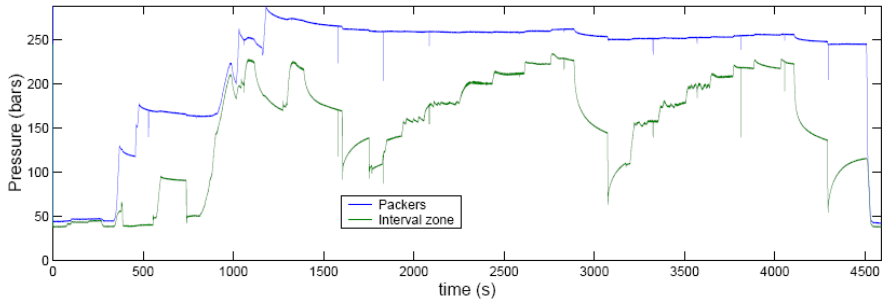

.